20123901 5A

別紙１

厚生労働科学研究費補助金

難病・がん等の疾患分野の医療の実用化研究事業

難治癌を標的治療できる完全オリジナルのウイルス遺伝子医薬の実用化のための前臨床研究

平成２４年度　総括・分担研究報告書

研究代表者　小戝　健一郎

平成２５（２０１３）年　５月

別紙２

目　　次

厚生労働科学研究費補助金（難病・がん等の疾患分野の医療の実用化研究事業）
総括研究報告書

研究総括

研究代表者　　小賀　健一郎　　鹿児島大学大学院医歯学総合研究科・教授

研究要旨

独自開発の「多因子での癌特異的増殖制御型アデノウイルス」(m-CRA)技術を基盤に、厚労科研（三次がん一期）で「既存技術を治療効果と安全性能で大きく凌ぐ Survivin 依存性 m-CRA (Surv.m-CRA)の開発」等、同（二期）で「癌幹細胞治療への Surv.m-CRA の応用」等の成果を上げてきた。この独自開発した画期的な癌治療医薬の Surv.m-CRA の治験開始のため、前臨床試験のデータ取得を３年間で行う。

研究分担者

三井　薫　　鹿児島大学大学院医歯学総合研究科・講師
前薗　理恵　鹿児島大学大学院医歯学総合研究科・助教
王　宇清　　鹿児島大学産学連携推進センター・プロジェクト研究員
伊地知　暢広鹿児島大学大学院医歯学総合研究科・助教
小宮　節郎　鹿児島大学大学院医歯学総合研究科・教授
永野　聡　　鹿児島大学大学院医歯学総合研究科・助教
夏越　祥次　鹿児島大学大学院医歯学総合研究科・教授

福崎　好一郎株式会社新日本科学・専務取締役

A．研究目的

独自開発の「多因子での癌特異的増殖制御型アデノウイルス」(m-CRA)技術を基盤に、厚労科研（三次がん一期）で「既存技術を治療効果と安全性能で大きく凌ぐ Survivin 依存性 m-CRA (Surv.m-CRA)の開発」等、同（二期）で「癌幹細胞治療への Surv.m-CRA の応用」等の成果を上げてきた。この独自開発した画期的な癌治療医薬の Surv.m-CRA の治験開始のため、前臨床試験のデータ取得を３年間で行う。

B．研究方法

① GLP/GMP製造と品質・安全性試験

Master viral bank(MVB)樹立、MVBの品質テスト、GMP製造法確立は既に行った。
前臨床試験用のGMPを委託で追加生産していく。

② 前臨床（非臨床）試験

POC(Proof of Concept)試験を鹿児島大学で対象癌に絞って1. In vitro試験（特異性検証）、2.in vivo試験（治療効果・用量探索試験）を行う
また、安全性試験として毒性試験な遺伝子ウイルス医薬の特殊試験は分担の新日本科学福崎やコンサルタント会社の助言指導の下、海外CROへ委託する。

C．研究結果

独自開発の m-CRA（多因子で癌特異化する増殖制御型アデノウイルスベクター）作製技術を基盤に開発した、Surv.m-CRA の医師主導治験開始に向け GMP 製造、非臨床試験、ならびに当局対応を計画通り行った。

① 医師主導治験のプロトコール案（概略）を検討し、作成した。それを基に治験用の GMP 製剤の製造、GLP 対応動物での非臨床試験等、全体の計画を立案した。
② 今回の治験薬となる Surv.m-CRA-1 の、臨床用の GMP 製剤の製造会社の選定を行った。国内には十分な実績を持つ会社がなかったため、

この遺伝子治療の分野で世界的な実績を持つ米国3施設の担当者との情報交換、そして現地視察を行った。その結果、以前に製造を受託して一部製造を行っている米国の会社を選定した。今年度はこの会社にて、ウイルスシードストックからのMaster virus bankの作製、治験用のGMP製剤の追加製造を行った。

③ 上記②と同様に、遺伝子治療という特殊な領域であるため、治験に準拠したGLPでの非臨床試験で十分な実績を持つ国内の会社がなかった。このため、この領域で世界的な実績を持つ米国2社、英国1社の担当者と情報交換をし、対応可能と判断される米国1社、英国1社の現地視察も行った。その結果、米国の会社を選定した。今年度はこの会社にて、まずはハムスターを用いた用量設定単回投与毒性試験を行った。その結果、ヒト患者での治験で予定している最大投与量の70倍の量でも、明らかな病的所見を生じなかった。また同社にてBiodistribution studyのために、定量PCRの方法確立とそのValidationを行った。この確立した定量PCRの手法でこの動物での投与後のSurv.m-CRA-1の生体内分布を解析した。

④ 全体の開発計画を各進行に伴い具体化し、併せてPMDA（独立行政法人医薬品医療機器総合機構）の個別面談、事前面談を行った。遺伝子治療医薬品の開発に係る一般的事項、非臨床安全性に係る一般的な事項だけでなく、本件で特に留意すべき事項として、1)動物種の選択、2)癌特異性について、3)投与経路について、4)臨床試験などについて、5)品質に関する事項など、具体的な助言と指導をもらい、今後の開発計画が具体化できた。

D．考察

本申請書研究は、単なる探索的臨床研究ではなく、（医師主導治験ではあるが）製剤承認に準じた治験に準拠して進めるものである。本申請で治験を行う予定の医薬は、以下の点より、革新医薬としての将来展望が期待できる。1) 治療効果と安全性の両性能が既存のCRAを既に凌駕しているという競合技術への優位性がある。2)癌幹細胞への強力な治療効果という、従来の治療法にない効果、従来の治療法が克服できなかった点を克服する能力を持つ製薬となるため、従来技術への高い優位性がある。3)最初の臨床試験の今回は単純なSurv.CRAで行うが、さらなる改良（m-CRA化）で治療効果や安全性が向上できることを科学的に実証しており、将来性が大きい。4)基本のベクター技術を持つため、さらに科学的に新しいm-CRA医薬を開発していること（複数を特許申請済み、論文準備中）、つまりこの分野で本邦初の本治験が成功すれば、後に続く科学的成果の治験の道筋もでき、本邦でのこの分野の科学研究から臨床応用の展望も開けることが期待できる。また複数のシーズがあり、さらに将来的にも次々に医薬シーズを創出できる基盤技術を持つことは、本申請で早期治験が成功できた場合、製薬企業へ技術移転が出来る可能性が大きい。5)ベクター作製の基本技術を基本特許として国内、国際特許も取得できているし、また関連する複数のm-CRA技術や医薬の特許も国際特許も含めて申請しているように、知財が極めて強力である。本申請での臨床試験は最終的な製剤化に繋がる治験として進めるため、知財が強力なシーズで治験基準での成果は、そのまま後期治験に進める貴重な成果となり、企業の後期治験に繋がると期待できる。このように知財の点から、海外のメガファーマも含めた製薬企業へ技術移転が出来る可能性が大きい。よって本研究の成果は、これまで通り、まず知財を確保し、論文や学会での学術的発表、あるいは市民公開講座などで社会にも発表し、そして日米のアカデミアや産業界とも情報交換をして深め臨床化を進める努力をしていく。

E．結論

独自開発のm-CRA（多因子で癌特異化する増殖制御型アデノウイルスベクター）作製技術を基盤に開発した、Surv.m-CRAの医師主導治験開始に向けGMP製造、非臨床試験、ならびに当局対応を計画通り行った。

F．健康危険情報

特になし。

G．研究発表

1.論文発表

1. Okabe Y, Takahashi T, Mitsumasu C, Kosai K, MD, Tanaka E, Matsuishi T.: Alterations of Gene Expression and Glutamate Clearance in Astrocytes Derived from an MeCP2-null Mouse Model of Rett Syndrome. ***PLoS ONE*** 7(4):e35354, 2012
2. Hino S, Sakamoto A, Nagaoka K, Anan K, Wang Y, Mimasu S, Umehara T, Yokoyama S, Kosai K, and Nakao M.: FAD-dependent lysine-specific demethylase-1 regulates cellular energy expenditure. ***Nat. Commun.*** 3, doi:10.1038/ncomms1755 (Open journal) (2012)
3. Nagao H, **Setoguchi T**, Kitamoto S, Ishidou Y, Nagano S, Yokouchi M, Abematsu M, Kawabata N, Maeda S, Yonezawa S, **Komiya S**.: RBPJ Is a Novel Target for Rhabdomyosarcoma Therapy. ***PLoS One.*** 2012;7(7):e39268.
4. Kawamura I., Maeda S., Imamura K., **Setoguchi**

T., Yokouchi M., Ishidou Y., **Komiya S.:** SnoN suppresses maturation of chondrocytes by mediating signal cross-talk between transforming growth factor-β and bone morphogenetic protein pathways. ***J Biol Chem.*** 2012;287(34):29101-13.

5. Tanaka M, **Setoguchi T**, Ishidou Y, Arishima Y, Hirotsu M, Saitoh Y, Nakamura S, Kakoi H, Nagano S, Yokouchi M, Kamizono J, **Komiya** S.: Pathological femoral fractures due to osteomalacia associated with adefovir dipivoxil treatment for hepatitis B: a case report. ***Diagn Pathol.*** 7:108. 2012
6. Kato T, Koriyama C, Khan N, Samukawa T, Yanagi M, Hamada T, Yokomakura N, Otsuka T, Inoue H, Sato M, Natsugoe S, Akiba S.: EGFR mutations and human papillomavirus in lung cancer. ***Lung Cancer.*** 78(2):144-7. 2012
7. Arigami T, Uenosono Y, Ishigami S, Hagihara T, Haraguchi N, Matsushita D, Yanagita S, Nakajo A, Okumura H, Hokita S, Natsugoe S.: Expression of stanniocalcin 1 as a potential biomarker of gastric cancer. ***Oncology.*** 83(3):158-64 . 2012
8. Hayashi T, Ding Q, Kuwahata T, Maeda K, Miyazaki Y, Matsubara S, Obara T, Natsugoe S, Takao S.: Interferon-alpha modulates the chemosensitivity of CD133-expressing pancreatic cancer cells to gemcitabine. ***Cancer Sci.*** 103(5):889-96. 2012
9. Ding Q, Yoshimitsu M, Kuwahata T, Maeda K, Hayashi T, Obara T, Miyazaki Y, Matsubara S, Natsugoe S, Takao S. Establishment of a highly migratory subclone reveals that CD133 contributes to migration and invasion through epithelial-mesenchymal transition in pancreatic cancer. ***Hum Cell.*** 25(1):1-8. 2012
10. Owaki T, Matsumoto M, Okumura H, Uchicado Y, Kita Y, Setoyama T, Sasaki K, Sakurai T, Omoto I, Shimada M, Sakamoto F, Yoshinaka H, Ishigami S, Ueno S, Natsugoe S.: Endoscopic ultrasonography is useful for monitoring the tumor response of neoadjuvant chemoradiation therapy in esophageal squamous cell carcinoma. ***Am J Surg***. 203(2):191-7. 2012

2.学会発表

1. Ken-ichiro Kosai: Development of conditionally replicating adenovirus specifically targeting and/or efficiently treating cancer stem cells. （国内、口演[English]）第 71 回日本癌学会学術総会、2012 年 9 月 19-21 日（札幌）

2. Kiyonori Tanoue, Yuqing Wang, Takao Setoguchi, Setsuro Komiya, Shoji Natusgoe, Ken-ichiro Kosai. :Survivin-Responsive Conditionally Replicating Adenovirus Efficiently Treats Rhabdomyosarcoma-Initiating Cells. （国内、口演[Japanese]）第 71 回日本癌学会学術総会、2012 年 9 月 19-21 日（札幌）

3. 小賀健一郎、三井薫、王宇清、高橋知之．ヒト ES/iPS 細胞での再生医療の課題を克服する独自のアデノウイルスベクターと発現技術の開発．（国内・パネルディスカッション）第 11 回日本再生医療学会総会、2012 年 6 月 12-14 日（横浜）

4. 田上聖徳、王宇清、池田美奈子、三井薫、瀬戸口啓夫、小宮節郎、夏越祥次、小賀健一郎．独自開発の増殖型アデノウイルスベクターで癌幹細胞は効果的に治療できる．（国内・ポスター）第 11 回日本再生医療学会総会、2012 年 6 月 12-14 日（横浜）

5. 三井薫、井手佳菜子、高山明子、小賀健一郎．増殖型アデノウイルスベクターを用いた安全なヒト ES/iPS 細胞治療の開発．（国内・口演）第 11 回日本再生医療学会総会、2012 年 6 月 12-14 日（横浜）

6. 小賀健一郎：癌の遺伝子異常を標的とした診断と治療の可能性．（国内・特別講演）第 175 回日本医学放射線学会九州地方会 2012 年 6 月 9-10 日（鹿児島）

7. Tanoue K, Wang Y, Ikeda M, Mitsui K, Setoguchi T, Komiya S, Natsugoe S, Kosai K. : Efficient treatment of Rhabdomyosarcoma-initiating cells by Survivin-responsive conditionally replicating adenovirus : Promising m-CRA strategy for treating cancer stem cells. （国際・ポスター）The American Society of Gene Therapy's 15h Annual Meeting, May 16-May 19, 2012 (Philadelphia, USA)

H．知的財産権の出願・登録状況（予定を含む。）

【特許出願】

1. シノビオリンプロモーターを含む増殖制御型ウイルスベクター
   発明者：小賀健一郎
   出願人：鹿児島大学
   国内出願：2012 年 8 月 23 日
   （特願 2012-184651）

2. ヒト ES/iPS 細胞における遺伝子発現方法
   発明者：小賀健一郎、三井薫、高橋知之
   出願人：鹿児島大学、久留米大学
   国内出願：2012 年 5 月 23 日
   （特願 2012-117128）

厚生労働科学研究費補助金（難病・がん等の疾患分野の医療の実用化研究事業）
分担研究報告書

研究分担者　三井　薫　鹿児島大学大学院医歯学総合研究科（遺伝子治療・再生医学）・講師
研究分担者　前薗　理恵　鹿児島大学大学院医歯学総合研究科（遺伝子治療・再生医学）・助教
研究分担者　伊地知　暢広　鹿児島大学大学院医歯学総合研究科（遺伝子治療・再生医学）・助教
研究分担者　王　宇清　鹿児島大学産学連携推進センター・プロジェクト研究員
研究分担者　小宮　節郎　鹿児島大学大学院医歯学総合研究科（整形外科学）・教授
研究分担者　夏越　祥次　鹿児島大学大学院医歯学総合研究科（消化器・乳腺甲状腺外科）・教授
研究分担者　永野　聡　鹿児島大学大学院医歯学総合研究科（整形外科学）・助教
研究分担者　福崎　好一郎　株式会社新日本科学・専務取締役

上記研究者の分担報告はすべて研究総括報告書に記載している。

別紙４

研究成果の刊行に関する一覧表

書籍

著者氏名	論文タイトル名	書籍全体の編集者名	書　籍　名	出版社名	出版地	出版年	ページ

雑誌

発表者氏名	論文タイトル名	発表誌名	巻号	ページ	出版年
Okabe Y, Takahashi T, Mitsumasu C, Kosai K, MD, Tanaka E, Matsuishi T	Alterations of Gene Expression and Glutamate Clearance in Astrocytes Derived from an MeCP2-null Mouse Model of Rett Syndrome	***PLoS ONE***	7	e35354	2012
Hino S, Sakamoto A, Nagaoka K, Anan K, Wang Y, Mimasu S, Umehara T, Yokoyama S, Kosai K, and Nakao M	FAD-dependent lysine-specific demethylase-1 regulates cellular energy expenditure	***Nat. Commun.***	3	758	2012
Tanaka M, Setoguchi T, Ishidou Y, Arishima Y, Hirotsu M, Saitoh Y, Nakamura S, Kakoi H, Nagano S, Yokouchi M, Kamizono J, Komiya S	Pathological femoral fractures due to osteomalacia associated with adefovir dipivoxil treatment for hepatitis B: a case report	***Diagn Pathol***	7	108	2012
Kawamura I, Maeda S, Imamura K, Setoguchi T, Yokouchi M, Ishidou Y, Komiya S	SnoN suppresses maturation of chondrocytes by mediating signal cross-talk between transforming growth factor-β and bone morphogenetic protein pathways	***J Biol Chem***	287	29101-29113	2012

Nagao H, Setoguchi T, Kitamoto S, Ishidou Y, Nagano S, Yokouchi M, Abematsu M, Kawabata N, Maeda S, Yonezawa S, Komiya S	RBPJ Is a Novel Target for Rhabdomyosarcoma Therapy	***PLoS One***	7	e39268	2012
Kato T, Koriyama C, Khan N, Samukawa T, Yanagi M, Hamada T, Yokomakura N, Otsuka T, Inoue H, Sato M, Natsugoe S, Akiba S	EGFR mutations and human papillomavirus in lung cancer	***Lung Cancer***	78	144-147	2012
Arigami T, Uenosono Y, Ishigami S, Hagihara T, Haraguchi N, Matsushita D, Yanagita S, Nakajo A, Okumura H, Hokita S, Natsugoe S	Expression of stanniocalcin 1 as a potential biomarker of gastric cancer	***Oncology***	83	158-164	2012
Hayashi T, Ding Q, Kuwahata T, Maeda K, Miyazaki Y, Matsubara S, Obara T, Natsugoe S, Takao S	Interferon-alpha modulates the chemosensitivity of CD133-expressing pancreatic cancer cells to gemcitabine	***Cancer Sci.***	103	889-896	2012
Ding Q, Yoshimitsu M, Kuwahata T, Maeda K, Hayashi T, Obara T, Miyazaki Y, Matsubara S, Natsugoe S, Takao S	Establishment of a highly migratory subclone reveals that CD133 contributes to migration and invasion through epithelial-mesenchymal transition in pancreatic cancer	***Hum Cell***	25	1-8	2012
Owaki T, Matsumoto M, Okumura H, Uchicado Y, Kita Y, Setoyama T, Sasaki K, Sakurai T, Omoto I, Shimada M, Sakamoto F, Yoshinaka H, Ishigami S, Ueno S, Natsugoe S	Endoscopic ultrasonography is useful for monitoring the tumor response of neoadjuvant chemoradiation therapy in esophageal squamous cell carcinoma	***Am J Surg***	203	191-197	2012

OPEN ACCESS Freely available online

PLoS one

Alterations of Gene Expression and Glutamate Clearance in Astrocytes Derived from an MeCP2-Null Mouse Model of Rett Syndrome

Yasunori Okabe[1,2], Tomoyuki Takahashi[1,3]*, Chiaki Mitsumasu[1,3], Ken-ichiro Kosai[1,3,4], Eiichiro Tanaka[1,2], Toyojiro Matsuishi[1,3]

1 Division of Gene Therapy and Regenerative Medicine, Cognitive and Molecular Research Institute of Brain Diseases, Kurume University, Kurume, Japan, **2** Department of Physiology, Kurume University of Medicine, Kurume, Japan, **3** Department of Pediatrics, Kurume University of Medicine, Kurume, Japan, **4** Department of Gene Therapy and Regenerative Medicine, Advanced Therapeutics Course, Kagoshima University Graduate School of Medical and Dental Sciences, Kagoshima, Japan

Abstract

Rett syndrome (RTT) is a neurodevelopmetal disorder associated with mutations in the methyl-CpG–binding protein 2 (MeCP2) gene. MeCP2-deficient mice recapitulate the neurological degeneration observed in RTT patients. Recent studies indicated a role of not only neurons but also glial cells in neuronal dysfunction in RTT. We cultured astrocytes from MeCP2-null mouse brain and examined astroglial gene expression, growth rate, cytotoxic effects, and glutamate (Glu) clearance. Semi-quantitative RT-PCR analysis revealed that expression of astroglial marker genes, including GFAP and S100β, was significantly higher in MeCP2-null astrocytes than in control astrocytes. Loss of MeCP2 did not affect astroglial cell morphology, growth, or cytotoxic effects, but did alter Glu clearance in astrocytes. When high extracellular Glu was added to the astrocyte cultures and incubated, a time-dependent decrease of extracellular Glu concentration occurred due to Glu clearance by astrocytes. Although the shapes of the profiles of Glu concentration versus time for each strain of astrocytes were grossly similar, Glu concentration in the medium of MeCP2-null astrocytes were lower than those of control astrocytes at 12 and 18 h. In addition, MeCP2 deficiency impaired downregulation of excitatory amino acid transporter 1 and 2 (EAAT1/2) transcripts, but not induction of glutamine synthetase (GS) transcripts, upon high Glu exposure. In contrast, GS protein was significantly higher in MeCP2-null astrocytes than in control astrocytes. These findings suggest that MeCP2 affects astroglial genes expression in cultured astrocytes, and that abnormal Glu clearance in MeCP2-deficient astrocytes may influence the onset and progression of RTT.

Citation: Okabe Y, Takahashi T, Mitsumasu C, Kosai K-i, Tanaka E, et al. (2012) Alterations of Gene Expression and Glutamate Clearance in Astrocytes Derived from an MeCP2-Null Mouse Model of Rett Syndrome. PLoS ONE 7(4): e35354. doi:10.1371/journal.pone.0035354

Editor: Nicoletta Landsberger, University of Insubria, Italy

Received October 26, 2011; **Accepted** March 14, 2012; **Published** April 20, 2012

Funding: This work was supported in part by a Grant-in-Aid for Scientific Research (C) and a Grant-in-Aid for Young Scientists (B) from the Japan Society for the Promotion of Science. The funders had no role in study design, data collection and analysis, decision to publish, or preparation of the manuscript.

Competing Interests: The authors have declared that no competing interests exist.

* E-mail: takahashi_tomoyuki@kurume-u.ac.jp

Introduction

Rett syndrome (RTT) is a neurodevelopmetal disorder that affects one in 15,000 female births, and represents a leading cause of mental retardation and autistic behavior in girls [1,2]. Mutations in the methyl-CpG–binding protein 2 (MeCP2) gene, located in Xq28, have been identified as the cause for the majority of clinical RTT cases [3]. Knockout mouse models with disrupted MeCP2 function mimic many key clinical features of RTT, including normal early postnatal life followed by developmental regression that results in motor impairment, irregular breathing, and early mortality [4,5,6]. MeCP2 dysfunction may thus disrupt the normal developmental or/and physiological program of gene expression, but it remains unclear how this might result in a predominantly neurological phenotype.

In several RTT mouse models, a conditional knockout that is specific to neural stem/progenitor cells or postmitotic neurons results in a phenotype that is similar to the ubiquitous knockout, suggesting that MeCP2 dysfunction in the brain and specifically in neurons underlies RTT [1,6,7]. Recent studies have demonstrated that mice born with RTT can be rescued by reactivation of neuronal MeCP2 expression, suggesting that the neuronal damage can be reversed [1,6]. In addition, several studies using in vitro cell culture systems also indicate that MeCP2 may play a role in processes of neuronal maturation including dendritic growth, synaptogenesis, and electrophysiological responses [1,7]. These data support the idea that MeCP2 deficiency in neurons is sufficient to cause an RTT-like phenotype. However, emerging evidence now indicates that MeCP2 deficiency in glia may also have a profound impact on brain function [8,9,10,11,12,13]. Brain magnetic resonance (MR) studies in MeCP2-deficient mice demonstrated that metabolism in both neurons and glia is affected [8]. Furthermore, in vitro co-culture studies have shown that MeCP2-deficient astroglia non-cell-autonomously affect neuronal dendritic growth [9,10]. In addition, MeCP2-deficient microglia cause dendritic and synaptic damage mediated by elevated glutamate (Glu) release [11]. Very recent studies have indicated that re-expression of MeCP2 in astrocytes of MeCP2-deficient mice significantly improves locomotion, anxiety levels, breathing patterns, and average lifespan, suggesting that astrocyte dysfunc-

tion may be involved in the neuropathology and characteristic phenotypic regression of RTT [13].

Astrocytes regulate the extracellular ion content of the central nervous systems (CNS); they also regulate neuron function, via production of cytokines, and synaptic function, by secreting neurotransmitters at synapses [14,15]. Moreover, a major function of astrocytes is efficient removal of Glu from the extracellular space, a process that is instrumental in maintaining normal interstitial levels of this neurotransmitter [16]. Glu is a major excitatory amino acid; excess Glu causes the degeneration of neurons and/or seizures observed in various CNS diseases [14,17]. RTT is also associated with abnormalities in Glu metabolism, but these findings are controversial due to the limitations of the experimental strategies used. Two studies have demonstrated that Glu is elevated in the cerebrospinal fluid (CSF) of RTT patients [18,19]. MR spectroscopy in RTT patients also revealed elevations of the Glu and Gln peak [20,21]. On the other hand, an animal MR study reported that the levels of Glu and Gln were decreased in a mouse model of RTT [8]. A more recent study indicated that MeCP2-null mice have reduced levels of Glu, but elevated levels of Gln, relative to their wild-type littermates [22]. Another study reported increased Gln levels and Gln/Glu ratios in Mecp2 mutant mice, but no decreases in Glu levels [23]. Although these in vivo studies have explored the hypothesis that the Glu metabolic systems might be altered in RTT, no solid conclusions have yet been reached [24,25].

In this study, we investigated the contribution of MeCP2 to the physiological function of astrocytes. Our studies demonstrate that MeCP2 is not essential for the growth and survival of astrocytes, but is involved in astrocytic Glu metabolism via the regulation of astroglial gene expression.

Results

Characterization of MeCP2-null astrocytes

It was recently reported that MeCP2 is normally present not only in neurons but also in glia, including astrocytes, oligodenrocytes, and microglia [9,10,11]. To determine the roles of MeCP2 in astrocytes, we cultured cerebral cortex astrocytes from both wild-type ($MeCP2^{+/y}$) and MeCP2-null ($MeCP2^{-/y}$) mouse brains (Fig. 1). MeCP2-null astrocytes exhibited a large, flattened, polygonal shape identical to that of the wild-type astrocytes, suggesting that normal patterns of cellular recognition and contact were present. Semi-quantitative RT-PCR using primer sets that specifically amplify two splice variants, Mecp2 e1 and e2, showed that control astrocytes expressed Mecp2 e1 and e2, whereas neither Mecp2 variant was detectable in MeCP2-null astrocytes (Fig. 1A). We further confirmed expression of MeCP2 by immunocytochemical staining of astrocytes. In control samples, almost all GFAP-positive cells exhibited clear nuclear MeCP2 immunoreactivity in astrocytes, but no immunoreactivity was observed in MeCP2-null astrocytes (Fig. 1B).

MeCP2 has been reported to be involved in regulation of astroglial gene expression [26,27]. Consistent with this, GFAP levels were significantly higher in MeCP2-null astrocytes (Fig. 1A). Similarly, the expression of S100β, another astrocyte maturation marker, was significantly upregulated by MeCP2 deficiency (fold change of control = 1.0, GFAP: 2.195±0.504, n = 4 each, $p<0.05$; S100β: 2.779±0.329, n = 4 each, $p<0.01$). These results show that MeCP2 deficiency upregulates astroglial gene expression in astrocytes.

To compare the growth of the wild-type and MeCP2-null astrocytes, we counted total cell number at each passage (Fig. 2A). As passage number increased, the cell growth rate decreased dramatically for both types of astrocytes, ultimately culminating in senescence. There was no significant difference in growth rate between the control and MeCP2-null astrocyte cultures. We then measured astrocyte proliferation via BrdU incorporation assay (Fig. 2B and Fig. S1). After 2 h of BrdU treatment, the proportions of BrdU-incorporating cells were similar in the control and MeCP2-null astrocytes (6.635±1.655% in control versus 6.774±2.272% in MeCP2-null astrocytes, n = 4 each, $p = 0.962$). These results suggest that the absence of MeCP2 did not affect the proliferation of astrocytes in our culture condition.

We also tested the cytotoxic effects of hydrogen peroxide (H_2O_2), ammonium chloride (NH_4Cl), and glutamate (Glu), on astrocytes in our culture (Fig. 2C–E). In cultures derived from both wild-type and MeCP2-null strains, cell viability decreased with increasing concentrations of H_2O_2 and NH_4Cl. In contrast, in our culture conditions, we observed virtually 100% viability of both the control and MeCP2-null astrocytes after 24 h incubation with 10 mM Glu. Glu-induced gliotoxic effects have been previously reported by Chen et al. (2000), and are probably due to distinct differences in culture conditions, specifically the presence of glucose [28]. These results showed that H_2O_2 and NH_4Cl had a similar effect in both strains of astrocytes. There was no significant difference in viability between the control and MeCP2-null astrocyte cultures, indicating that MeCP2 deficiency did not affect astrocyte viability upon treatment with H_2O_2 and NH_4Cl.

Effects of glutamate on glutamate transporters and glutamine synthetase transcripts in MeCP2-null astrocytes

High extracellular Glu interferes with the expression of the astrocyte transporter subtypes, excitatory amino acid transporter 1(EAAT1)/glutamate/aspartate transporter (GLAST) and EAAT2/glutamate transporter-1 (GLT-1) [16,29]. To explore the effects of Glu on the expression of Glu transporter genes in cultured astrocytes from wild-type and MeCP2-null mouse brains, we asked whether treatment with 1.0 mM Glu altered expression of EAAT1 and EAAT2 mRNA, using a semi-quantitative RT-PCR assay (Fig. 3). EAAT1 and EAAT2 mRNA were expressed in both wild-type and MeCP2-null astrocytes, and were slightly higher in controls than in MeCP2-null astrocytes. Both EAAT1 and EAAT2 mRNA levels were altered in the control astrocytes after treatment with 1.0 mM Glu. EAAT1 mRNA levels decreased significantly in the wild-type astrocytes, both 12 h and 24 h after treatment with Glu (Fig. 3A). In contrast, EAAT1 decreased significantly in the MeCP2-null astrocytes, at 12 h but not 24 h after treatment. As with EAAT1, EAAT2 mRNA levels also decreased significantly in the control astrocytes, both 12 h and 24 h after treatment (Fig. 3B). However, EAAT2 decreased significantly in MeCP2-null astrocytes, 24 h but not 12 h after treatment. In addition, the effects of Glu on EAAT1 and EAAT2 relative fold expression at 12 h were altered in the MeCP2-null astrocytes (Fig. 3D: EAAT1; 0.618±0.033 in control versus 0.758±0.049 in MeCP2-null astrocytes, n = 10 each, $p<0.05$; Fig. 3E: EAAT2; 0.794±0.055 in control versus 0.964±0.048 in MeCP2-null astrocytes, n = 8 each, $p<0.05$). These results suggest that the loss of MeCP2 leads to transcriptional dysregulation of these genes, either directly or indirectly.

One important enzyme that plays a role in the Glu metabolic pathway is glutamine synthetase (GS) [17,29]. GS is mainly located in astrocytes; cultured astrocytes response to Glu with increased GS expression [17,29]. Consistent with this, 1.0 mM Glu treatment stimulated GS mRNA expression in both the wild-type and MeCP2-null astrocytes about 1.2-fold after 12 h but not 24 h (Fig. 3C). In addition, MeCP2 deficiency did not modify the

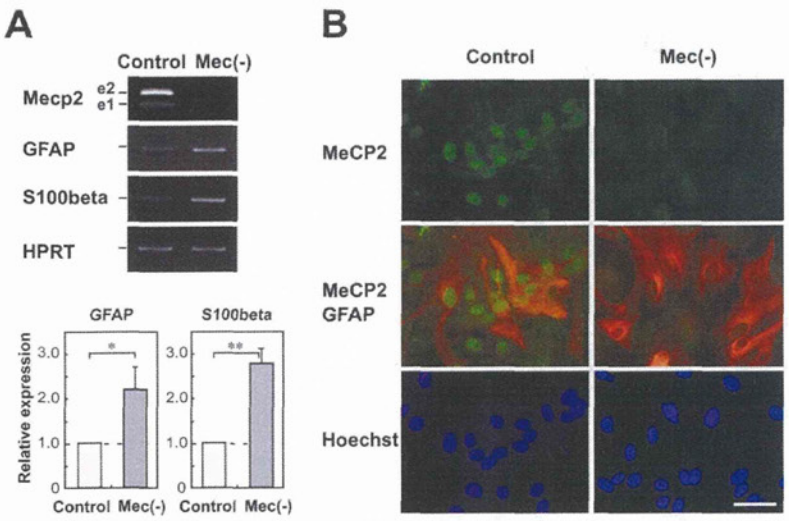

Figure 1. Characterization of assay cultures. A. Expression of astroglial genes in primary cultured cortical astrocytes. Semi-quantitative RT-PCR analysis of Mecp2 and astroglial genes was performed in wild-type (white column) and MeCP2-null (gray column) astrocytes. Mecp2 e1 and e2 were detectable in the wild-type astrocytes. The lower graphs show that the GFAP/HPRT or S100β/HPRT expression ratio in each genotype was normalized against the level in control astrocytes. Bars represent the means ± standard errors (SE) of samples from three independent experiments (*$p<0.05$). The expression of astroglial markers was significantly upregulated by MeCP2 deficiency. **B.** Expression of MeCP2 in the primary cultured cortical astrocytes. The astrocytes were immunostained with MeCP2 (green) and GFAP (red) as glial-specific astrocytic markers. Scale bars indicate 50 μm.
doi:10.1371/journal.pone.0035354.g001

effects of Glu on GS mRNA relative fold expression in cultured astrocytes (Fig. 3F, 1.245±0.054 in control versus 1.265±0.093 in MeCP2-null astrocytes, n = 6 each, p = 0.859). These results suggested that MeCP2 did not modify the expression of GS in the cultured astrocytes. Overall, the expression levels of GS mRNA did not differ between both strains of astrocytes following treatment with Glu.

Comparison of glutamate clearance between wild-type and MeCP2-null astrocytes

Because MeCP2 contributed to the transcriptional regulation of Glu metabolism-related genes in our culture systems, we next compared the Glu clearance capability of the wild-type and MeCP2-null astrocytes (Fig. 4A). The cell culture supernatants in both astrocyte cultures were collected at 3–24 h post incubation in culture media containing 1.0 mM Glu. After incubation in culture medium containing Glu, we identified a time-dependent reduction in Glu over 24 h of incubation in both strains of astrocytes. Although the shapes of the profiles of Glu concentration versus time for each strain of astrocytes were grossly similar, Glu concentration in the medium of MeCP2-null astrocytes were lower than those of control astrocytes at 12 and 18 h (12 h: control, 0.513±0.052 mM versus MeCP2-null, 0.395±0.022 mM, $p<0.05$; 18 h: control, 0.368±0.029 mM versus MeCP2-null, 0.125±0.007 mM, $p<0.01$, n = 6 each, Fig. 4A). The differences in Glu clearance were not due to changes in cell death of control astrocytes upon application of Glu (Fig. 2E). This indicates that Glu clearance by MeCP2-null astrocytes was more efficient than by control astrocytes.

The Glu transporters EAAT1 and EAAT2 are located primarily on astrocytes and are critical in maintaining extracellular Glu at safe levels [16]. Threo-beta-benzyloxyaspartate (TBOA) is a broad-spectrum glutamate transporter antagonist, affecting EAAT1 and EAAT2 [30]. UCPH-101 (2-amino-4-(4-methoxyphenyl)-7-(naphthalen-1-yl)-5-oxo-5,6,7,8-tetrahydro-4H-chromene-3-carbonitrile) and dihydrokainate (DHKA) are selective inhibitors for EAAT1 and EAAT2, respectively [30,31]. To investigate the functional Glu transporters in our astrocyte cultures, we analyzed three Glu transporter blockers (TBOA, UCPH-101, or DHKA) for their ability to alter the effects of Glu clearance (Fig. 4B–D). Glu clearance by the wild-type astrocytes was partially blocked by addition of TBOA and UCPH-101, but not DHKA. This suggests that EAAT1, but not EAAT2, plays a major role in Glu clearance under our astroglial culture conditions.

Effects of glutamate on glutamine synthetase and EAAT1 protein in MeCP2-null astrocytes

The initial set of experiments aimed to determine whether Glu modulate the translation of GS and EAAT1 protein (Fig. 5 and Fig. S2). GS protein was expressed in both wild-type and MeCP2-null astrocytes, and was significantly more abundant in MeCP2-null astrocytes (Fig. 5B: fold change of control = 1.0, 2.631±0.368, $p<0.01$). After 12 h exposure to 0.01–1.0 mM Glu, wild-type astrocytes exhibited a dose-dependent increase in GS protein levels (about 6-fold in 1.0 mM Glu treatment). Similar to its effect on the wild-type astrocytes, in the MeCP2-null astrocytes Glu exposure dose-dependently increased GS protein levels relative to untreated astrocytes (Fig. S2). We then examined the effect of 1.0 mM Glu on levels of GS protein, over a time course (Fig. 5A). GS expression was highest after 12 h exposure to 1.0 mM Glu, decreasing slightly by 24 h in both wild-type and MeCP2-null astrocytes. Densitometric analysis of the bands in three independent experiments demonstrated that GS protein in MeCP2-null astrocyte cultures was higher than in wild-type astrocytes, 12 h but not 24 h after treatment (Fig. 5B: fold change of control = 1.0, at 12 h: 1.421±0.139, $p<0.05$; at 24 h: 1.131±0.130, p = 0.354, n = 4 each). These results indicated that MeCP2 deficiency caused higher expression of GS protein in cultured astrocytes.

We also asked whether treatment with 1.0 mM Glu altered expression of EAAT1 protein. EAAT1 protein was expressed in

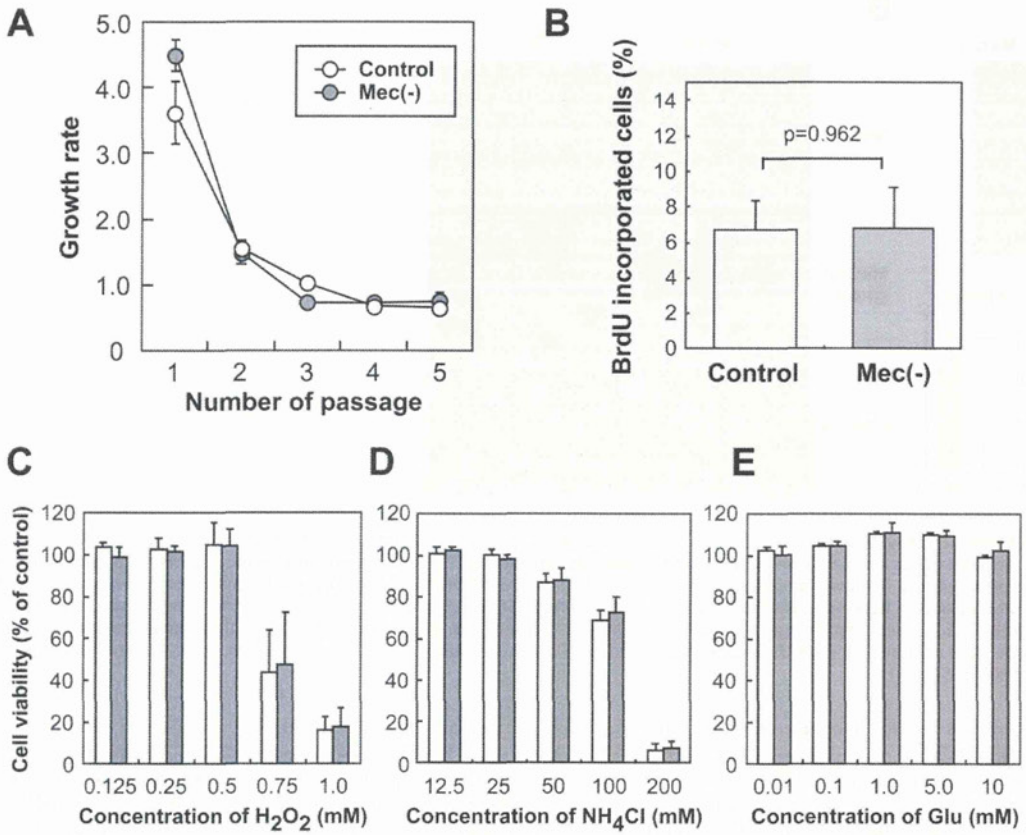

Figure 2. Cell growth and viability. A. Comparison of cell growth in wild-type and MeCP2-deficient astrocytes. As passage number increased, cell growth rate decreased dramatically in both strains of astrocytes. There was no significant difference in growth rate between the control and MeCP2-null astrocyte cultures. **B.** Quantification of BrdU-incorporating cells in control and MeCP2-null astrocytes. Astrocytes were cultured for 24 h and incubated with BrdU for 2 h. The graph shows the percentage of BrdU-incorporating cells in the control (white column) and MeCP2-deficient (gray column) astrocytes 2 h after BrdU exposure. The number of BrdU-incorporating cells is expressed as a percentage of the total number of Hoechst-stained cells (Fig. S1). Bars represent the means ± SE of the samples from four independent experiments. The ratio of BrdU-incorporating cells is similar in astrocytes taken from both control and MeCP2-null strains. **C–E.** Comparison of effects of various neurotoxins (**C,** H_2O_2; **D,** NH_4Cl; **E,** Glutamate) on control and MeCP2-null astrocytes. The graph shows the percentage of viability in the control (white column) and MeCP2-deficient (gray column) astrocytes after neurotoxin treatment at the indicated concentrations. Bars represent the means ± SE of samples from three independent experiments. The glial cultures showed no difference in viability between the control and MeCP2-null strains.
doi:10.1371/journal.pone.0035354.g002

both wild-type and MeCP2-null astrocytes, at levels that were similar in controls and MeCP2-null astrocytes. EAAT1 protein levels were altered in the wild-type astrocytes after treatment with 1.0 mM Glu. EAAT1 protein levels decreased significantly in the wild-type astrocytes, 24 h but not 12 h after treatment (Fig. 5C). In contrast, EAAT1 did not decrease in the MeCP2-null astrocytes, either 12 h or 24 h after treatment. In addition, the relative expression levels of EAAT1 24 h after treatment were lower in the wild-type than in the MeCP2-null culture, although the difference was not statistically significant (Fig. 5D: 12 h; 1.102±0.169 in control versus 1.096±0.142 in MeCP2-null astrocytes, n = 6 each, p = 0.979, 24 h; 0.456±0.123 in control versus 0.901±0.172 in MeCP2-null astrocytes, n = 5 each, p = 0.068). These results suggest that MeCP2 deficiency affects the expression of GS and EAAT1 protein, and that accelerated Glu clearance may result from dysregulation of GS and EAAT1 protein in MeCP2-null astrocytes.

Discussion

Recent studies suggest that glia, as well as neurons, cause neuronal dysfunction in RTT via non-cell-autonomous effects. Here, we have demonstrated that MeCP2 regulates the expression of astroglial marker transcripts, including GFAP and S100β in cultured astrocytes. In addition, MeCP2 is not essential for the cell morphology, growth, or viability; rather, it is involved in Glu clearance through the regulation of Glu transporters and GS in astrocytes. Altered astroglial gene expression and abnormal Glu clearance by MeCP2-null astrocytes may underlie the pathogenesis of RTT.

In this study, MeCP2-null astrocytes exhibited significantly higher transcripts corresponding to astroglial markers, including GFAP and S100β. Consistent with this, transcription of several astrocytic genes, including GFAP, is upregulated in RTT patients [26,32]. Indeed, MeCP2 binds to a highly methylated region in the GFAP and S100β in neuroepithlial cells [27,33]; ectopic

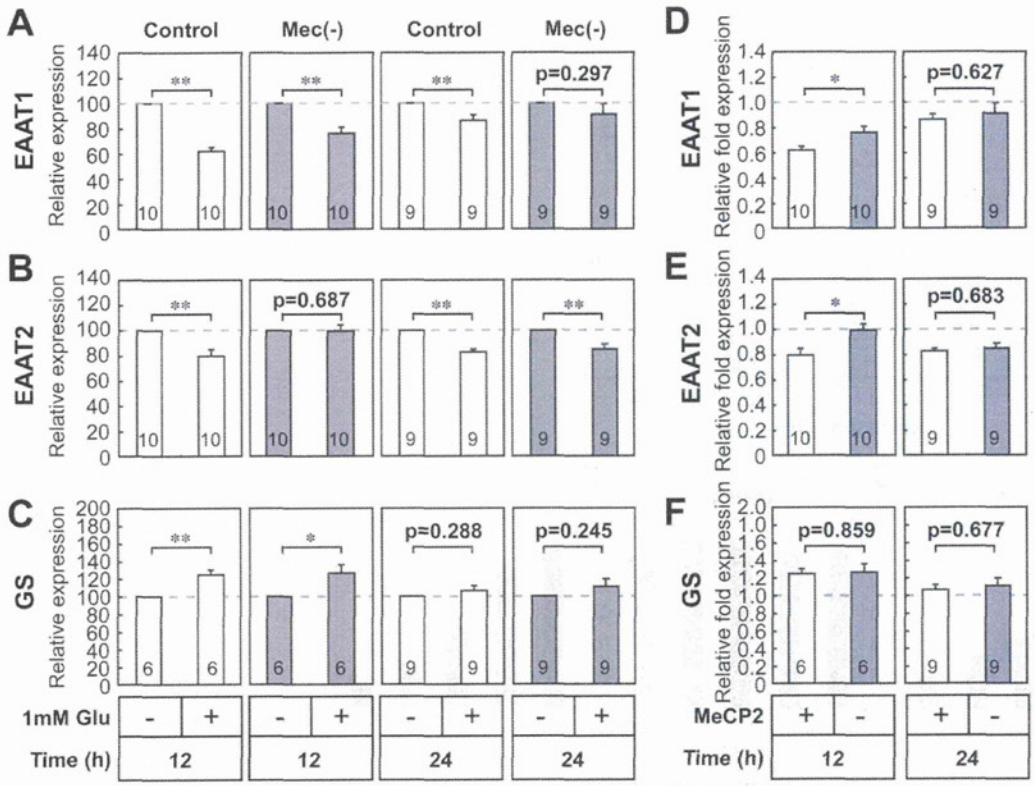

Figure 3. Effect of glutamate on glutamine synthetase and glutamate transporter gene expression in MeCP2-null astrocytes. A–C. Effects of Glu on Glu clearance-related genes in wild-type (white column) and MeCP2-null (gray column) astrocytes. Semi-quantitative RT-PCR analysis of Glu clearance-related genes, EAAT1 (**A**), EAAT2 (**B**), and GS (**C**), was performed in the control and MeCP2-null astrocytes 12 or 24 h after treatment with 1.0 mM Glu. The bands corresponding to PCR products were quantified by densitometry, normalized against HPRT levels, and expressed as % of controls (equals 100%). Bars represent the means ± SE of samples from 3–4 independent experiments (*$p<0.05$, **$p<0.01$). **D–F.** Comparison of the effects of Glu on EAAT1, EAAT2 or GS expression in the control and MeCP2-null astrocytes. The ratio of EAAT1/HPRT (**D**), EAAT2/HPRT (**E**) or GS/HPRT (**F**) in each treatment group was normalized against that of the non-treated astrocytes from each group. Bars represent the means ± SE of samples from 3–5 independent experiments (*$p<0.05$). Numbers in each column indicate the total number of samples analyzed.
doi:10.1371/journal.pone.0035354.g003

overexpression of MeCP2 inhibited the differentiation of neuroepithelial cells into GFAP-positive glial cells [34]. Our recent study in RTT-model ES cells also demonstrated that MeCP2 is involved in gliogenesis during neural differentiation via inhibition of GFAP expression [12]. Therefore, MeCP2 may be involved not only in the suppression of astroglial genes in neuroepithelial cells/neurons during neurogenesis, but also in the physiological regulation of astroglial gene expression in astrocytes.

We also demonstrated that MeCP2 is not essential for cell growth or cell viability in in vitro models of astrocyte injury, such as H_2O_2 oxidative stress and ammonia neurotoxicity. On the other hand, it has been reported that MeCP2 is involved in regulating astrocyte proliferation, and are probably due to distinct differences in culture conditions, specifically the presence of serum [10]. Consistent with these results, obvious neuronal and glial degeneration had not been observed in RTT [6,35]. These observations suggest that RTT is not caused by reduced cell numbers, but rather by dysfunction of specific cell types in the brain.

The regulation of Glu levels in the brain is an important component of plasticity at glutamatergic synapses, and of neuronal damage via excessive activation of Glu receptors [15,16]. Astrocytic uptake of Glu, followed by conversion of Glu to Glutamine (Gln), is the predominant mechanism of inactivation of Glu once it has been released in the synaptic cleft. This uptake involves two transporters, EAAT1/GLAST and EAAT2/GLT-1 [16]. Increases in extracellular Glu, present in many brain injuries, are sufficient to modulate the expression of Glu transporters and GS [16,29]. Furthermore, application of 0.5–1.0 mM Glu to cultured cortical astrocytes causes a decline in EAAT1/GLAST and EAAT2/GLT-1 expression [29]. Our present studies reveal that 1.0 mM extracellular Glu is sufficient to inhibit astroglial Glu transporter expression and to stimulate GS expression in control astrocytes. However, such regulatory influences on Glu transporters are impaired by MeCP2 deficiency. Therefore, MeCP2 may regulate the expression of Glu transporters under physiological conditions. Currently, little is known about the promoter regions of the main Glu transporters [36,37]. Promoter analysis in each gene may help to elucidate the complex regulations of astroglial genes by MeCP2.

On the other hand, in our culture conditions, MeCP2 deficiency did not impair the expression of GS transcripts in cultured astrocytes, but did affect the expression of GS protein. A very recent study has shown that defects in the AKT/mTOR pathway

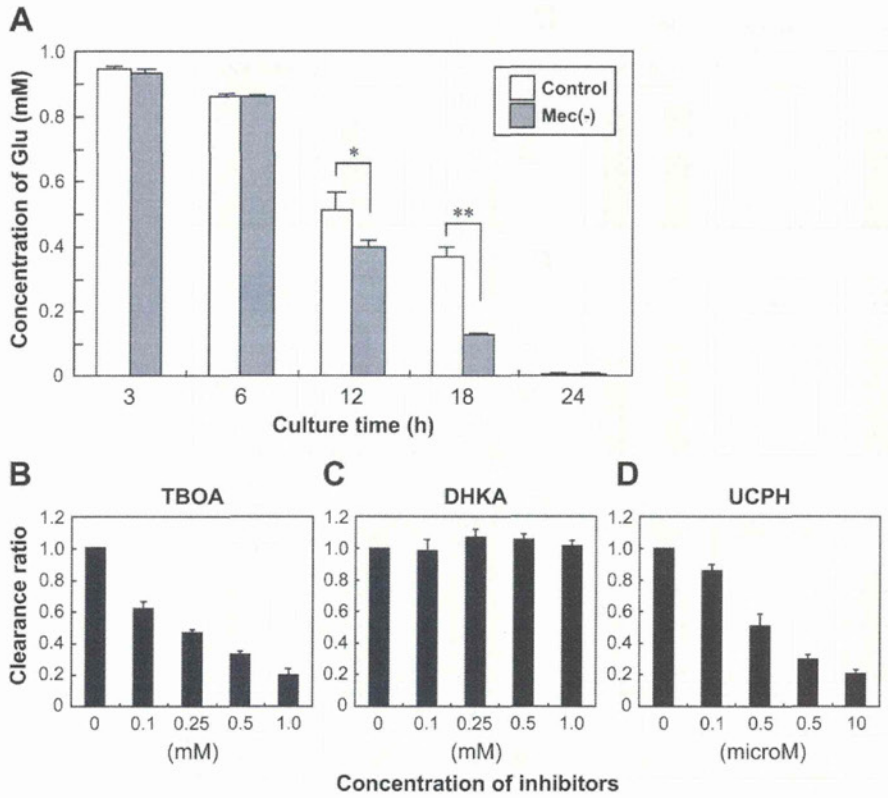

Figure 4. Comparison of glutamate clearance in wild-type and MeCP2-null astrocytes. A. Time-dependent reduction of extracelluar Glu concentration in wild-type (white column) and MeCP2-null (gray column) astrocyte cultures. After treatment with 1.0 mM Glu, culture supernatant was collected at the indicated times for the determination of Glu concentration. The graph shows the concentration of Glu in control and MeCP2-null astrocyte culture medium. Bars represent the means ± SE of samples from three independent experiments (*$p<0.05$). **B–D.** Effects of inhibitors of glutamate transporters (**B,** TBOA; **C,** DHKA; **D,** UCPH) on Glu clearance. Astrocytes were exposed to the indicated concentration of Glu transporter inhibitors, and then 0.1 mM Glu was added; culture supernatant was collected for the determination of Glu concentration at 2 h. The graphs show the clearance ratio upon treatment with each inhibitor. The clearance ratio in the indicated concentration groups was expressed by defining the control level (no inhibitor) as 1.0. Bars represent the means ± SE of samples from three independent experiments.
doi:10.1371/journal.pone.0035354.g004

are responsible for altered translational control in MeCP2 mutant neuron [38]. These findings suggest that a deficit in protein synthesis and/or turnover in the MeCP2-null astrocytes might influence the final levels of GS protein. Further studies are necessary to investigate whether MeCP2 deficiency impairs the synthesis and turnover of proteins in RTT.

The most important finding in this study was that MeCP2 deficiency in astrocytes accelerates Glu clearance. Consistent with this, RTT is associated with abnormalities in the Glu metabolism [24]. Some studies have demonstrated increases in Glu levels in the cerebrospinal fluid (CSF) of human RTT patients [18,19]. On the other hand, in animal studies there have been instances of decreased Glu levels and/or Glu/Gln ratios, as determined by in MR spectroscopy [8,21,22,23]. Furthermore, MeCP2-deficient microglia release an abnormally high level of Glu, causing excitotoxicity that may contribute to dendritic and synaptic abnormalities in RTT [11]. These results clearly suggest that MeCP2 has the potential to regulate Glu levels in the brain under certain circumstances. Glu levels are altered in the RTT brain, but the mechanisms responsible for the changes in Glu metabolism are unknown. In light of our findings, we speculate that abnormal expression of Glu transporters and GS resulting from MeCP2 deficiency could lead to abnormal Glu clearance in astrocytes and in turn to altered levels of Glu in RTT brain. Additional studies are needed to determine the mechanisms underlying changes in Glu levels and Glu metabolism, and their role in the RTT brain.

In conclusion, MeCP2 modulates Glu clearance through the regulation of astroglial genes in astrocytes. This study suggests a novel role for MeCP2 in astrocyte function; these findings may be useful in exploration of a new approach for preventing the neurological dysfunctions associated with RTT.

Materials and Methods

Cell culture

For each experiment, primary cultures were generated from individual MeCP2-null neonates and their wild-type littermates; tail snips from each neonate were obtained for genotyping, as described below. Enriched cultures of GFAP-expressing astroglial cells, which are virtually free of neurons and microglial cells, were established from the cerebral hemispheres of postnatal day (P) 0 to P1 newborn mice, as previously described [29]. In brief, pieces of dissected tissue were trypsinized (0.05%) for 10 min in Ca_2^+- and Mg_2^+-free phosphate-buffered saline (PBS) supplemented with

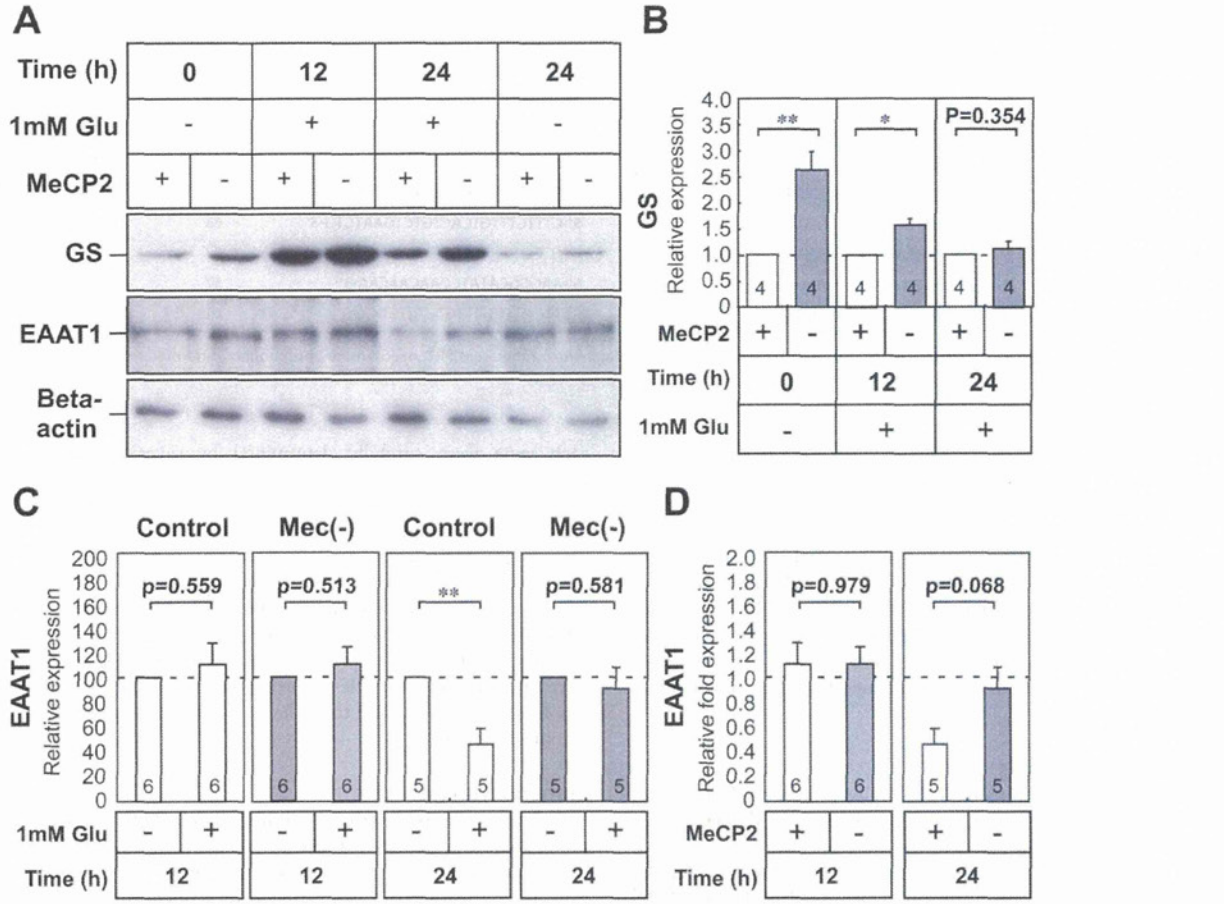

Figure 5. Effect of glutamate on glutamine synthetase and EAAT1 protein expression in MeCP2-null astrocytes. A. Time-dependent expression of GS and EAAT1 proteins in wild-type and MeCP2-deficient astrocyte cultures. Astrocytes were treated with 1.0 mM Glu for 24 h, and subsequently analyzed for expression of GS and EAAT1 by Western blot analysis. Beta-actin protein levels were analyzed in the same way, as an internal control. **B.** The immunoreactive GS protein bands were quantified by densitometry, normalized against β-actin levels, and expressed as fold change relative to the controls (equals 1.0). Bars represent the means ± SE of samples from three independent experiments (*$p<0.05$, **$p<0.01$). Numbers in each column indicate the total number of samples analyzed. **C.** The immunoreactive EAAT1 protein bands were quantified by densitometry, normalized against β-actin levels, and expressed as % of controls (equals 100%). Bars represent the means ± SE of samples from three independent experiments (**$p<0.01$). **D.** Comparison of the effects of Glu on EAAT1 expression in wild-type and MeCP2-null astrocytes. The ratio of EAAT1/β-actin in each treatment group was normalized against that of the non-treated astrocytes from each group. Bars represent the means ± SE of samples from three independent experiments. Numbers in each column indicate the total number of samples analyzed.
doi:10.1371/journal.pone.0035354.g005

0.02% EDTA. Tissue samples were subsequently dissociated in Hank's balanced salt solution (HBSS) containing 15% fetal calf serum (FCS; F2442, Sigma-Aldrich, Inc., St. Louis, MO, USA) by trituration though 10-ml plastic pipettes. Cells were pelleted at 100×g for 5 min, resuspended in Dulbecco's modified Eagle's medium (D-MEM; Wako Pure Chemical Industries, Ltd., Osaka, Japan) containing 15% FCS, and seeded into 100-mm culture dishes previously coated with poly-D-lysine (0.1 mg/ml; Wako Pure Chemical Industries, Ltd., Osaka, Japan). Upon reaching confluency, cells were trypsinized and replated. Cells were used after the third passage (P3) in all experiments, and were seeded at 3×10^4 cells/cm^2 in 6-well plate dishes or 35-mm culture dishes. Cultures were assayed by immunochemical analysis using antibodies against GFAP, MAP2, and CD11b in order to determine the degree of enrichment; the astrocyte cultures were nearly pure without contamination of microglia and neurons (Fig. S3 and Information S1).

Cell growth and bromo-2′-deoxyuridine (BrdU) uptake assay

To determine growth rate, cells were plated at 2×10^5 cells/dish in 35-mm dishes. At each passage, three dishes per cell line were harvested by trypsinization, and cell numbers were determined using a hemocytometer. Growth rate was expressed as the number of harvested cells divided by the number of seeded cells.

BrdU incorporation during DNA synthesis was determined using the 5-Bromo-2′-deoxy-uridine Labeling and Detection Kit I (Roche, Indianapolis, IN, USA). Briefly, cells were seeded at 3.0×10^4 cells per well in 48-well culture plates and incubated in D-MEM containing 10% FCS at 37°C for 24 h. After cells were

Table 1. PCR primers.

	Sense	Antisense	Ta	cycles
GFAP	5′-ATCCGCTCAGGTCATCTTACCC-3′	5′-TGTCTGCTCAATGTCTTCCCTACC-3′	63	25
S100β	5′-AGAGGACTCCAGCAGCAAAGG-3′	5′-AGAGAGCTCAGCTCCTTCGAG-3′	59	32
EAAT1	5′-GAAGTCTCCCAGACGTTCTAATCC-3′	5′-GCTCTGAAACCGCCACTTACTATC-3′	65	35
EAAT2	5′-ATGCTCATCCTCCCTCTTATCATC-3′	5′-CTTTCTTTGTCACTGTCTGAATCTG-3′	63	32
GS	5′-TGTACCTCCATCCTGTTGCC-3′	5′-GTCCCCGTAATCTTGACTCC-3′	57	25
HPRT	5′-CCTGCTGGATTACATTAAAGCACTG-3′	5′-AAGGGCATATCCAACAACAA-3′	57	30
MeCP2	5′-GGTAAAACCCGTCCGGAAAATG-3′	5′-TTCAGTGGCTTGTCTCTGAG-3′	61	35

GFAP, glial fibrillary acidic protein; EAAT, excitatory amino acid transporter; GS, glutamine synthetase; HPRT, hypoxantine-phosphoribosyl-transferase; MeCP2, methyl-CpG-binding protein 2; Ta, annealing temperature (°C).

doi:10.1371/journal.pone.0035354.t001

incubated with 10 μM BrdU for 2 h, they were fixed with 70% ethanol in 50 mM glycine (pH 2.0) for 20 min at −20°C. Cells were incubated with an anti-BrdU monoclonal antibody, followed by a fluorescein-coupled goat anti-mouse Ig and Hoechst33324 (1 μg/ml). To determine the percentages of BrdU-positive cells, fluorescent images were obtained by a Biorevo BZ-9000 fluorescence microscope (KEYENCE Co., Osaka, Japan); images were analyzed using the BZ-II application. BrdU-positive cells and total cells were counted in random 3 fields per well (approximately 1200 cells per well). Results were obtained from four independent experiments.

Cell Viability Analysis

Cell were seeded at 1×10^4 cells per well in 96-well plates and incubated in D-MEM containing 15% FCS at 37°C for 24 h. In injury models of drug and oxidative stress, cells were incubated with 0.01–10 mM glutamate for 24 h, 12.5–200 mM NH_4Cl (Sigma Chemical Co.) for 4 h, or 0.125–1.0 mM H_2O_2 (Wako Pure Chemical Industry, Osaka, Japan) for 1 h as previously described [28,39,40]. After 24 h of drug treatment, cell viability was determined using the WST-8 assay (NACALAI TESQUE, INC., Kyoto, Japan) [39,41].

PCR analysis

MeCP2$^{-/+}$ female mice (B6.129P2(C)-Mecp2$^{tm1.1Bird}$/J strain) were purchased from the Jackson Laboratory (Bar Harbor, ME) and mated with wild-type C57BL/6 male mice. DNA samples were extracted from tail snips from newborn animals; prior to nucleic acid extraction, snips were digested with proteinase K. Genotyping was performed by PCR analysis of genomic DNA according to the protocol provided by the manufacturer (http://jaxmice.jax.org/pub-cgi/protocols/protocols.sh?objtype=protocol&protocol_id=598) [4,12]. All experiments were performed in accordance with the National Institutes of Health Guidelines for the Care and Use of Laboratory Animals, and were approved by the Animal Research Committee of Kurume University.

Total RNA was extracted from cells using a Sepazol RNA I super kit (Nacalai Tesque, Inc., Kyoto, Japan) [41,42]. One microgram of total RNA was reverse transcribed, and 1/100 of the cDNA (equivalent to 10 ng of total RNA) was subjected to PCR amplification with Taq DNA polymerase (Promega, Co., Ltd., Madison, WI) using the following conditions: 25–35 cycles of 94°C for 30 s, annealing temperature for 60 s, and 74°C for 60 s. Primer sets and annealing temperatures are shown in Table 1. The most appropriate PCR conditions for semi-quantitative analysis of each gene were carefully determined by several preliminary experiments (Fig. S4). The number of cycles for GFAP, S100β, EAAT1, EAAT2, and GS was 25, 32, 35, 32, and 25, respectively (Table 1). The amplified cDNA was electrophoresed on 2% agarose gels containing ethidium bromide, and quantities were analyzed by densitometry using ImageJ software (the Research Service Branch of the National Institute of Health, Bethesda, MD, USA) [42]. The relative expression of each gene was normalized to the intensity of a housekeeping gene, hypoxantine-phosphoribosyl-transferase (HPRT; 30 cycles). The expression level of each gene is reported as a ratio relative to the level of normalized expression in a control sample.

Immunocytochemistry

Cultures were fixed with 4% paraformaldehyde for 10 min and permeabilized with 0.05% Triton-X 100 for 5 min. After blocking of nonspecific binding sites with 10% nonfat dry milk in PBS for 1 h, cultures were immunocytochemically stained using antibodies against MeCP2 (anti-MeCP2 polyclonal antibody, MILLIPORE, Temecula, CA, USA; anti-MeCP2 monoclonal antibody, G-6, Santa Cruz Biotechnology, Inc., Santa Cruz, CA), β-tubulin type III (TuJ, Sigma-Aldrich, Inc., St. Louis, Missouri), or glial fibrillary acidic protein (GFAP) (anti-GFAP polyclonal antibody, G9269; anti-GFAP monoclonal antibody, G3893, Sigma-Aldrich, Inc., St. Louis, Missouri), followed by secondary fluorescent antibodies as described previously [12]. Cultures were additionally stained with Hoechst33342 and examined using an Olympus IX-70 (Olympus Japan Inc. Tokyo, Japan) microscope. Photomicrographs were captured using an Olympus DP70 digital camera.

Immunoblotting

Cell extracts were prepared from astroglial cultures as described previously [41]. Western blot analysis was performed using anti-glutamine synthetase (G2781; Sigma-Aldrich, Inc., St. Louis, Missouri), anti-excitatory amino acid transporter 1 (EAAT1, GLAST; Santa Cruz Biotechnology, Inc., Santa Cruz, CA), horseradish peroxidase-conjugated anti-rabbit IgG (DakoCytomation, Glostrup, Denmark), and chemiluminescent substrate (Chemi-Lumi One, NACALAI TESQUE, INC., Kyoto, Japan) [12,41]. Several different exposure times were used for each blot to ensure linearity of band intensities. Immunoreactive bands were quantified using the ImageJ software (Research Service Branch of the National Institute of Health, Bethesda, MD, USA). The relative expression of each protein was normalized to the intensity of β-actin. The expression level of each protein is reported as a

ratio relative to the level of normalized expression in a control sample.

Glutamate Clearance Assay

To measure extracellular glutamate (Glu) concentrations, we used the Glutamate Assay Kit colorimetric assay (Yamasa Corporation, Tokyo, Japan) [43]. Assays were carried out in six independent trials. The clearance ratio of Glu was calculated from the Glu concentration (μM) in the medium sample of the drug-treated astroglial cells (Glu_{drug}) and the control non-drug treated (i.e., treated with drug vehicle alone) glial cells (Glu_{solv}). This is represented mathematically as follows: Glu clearance ratio = $(100-Glu_{drug})/(100-Glu_{solv})$. Threo-beta-benzyloxyaspartate (TBOA), UCPH-101 (2-amino-4-(4-methoxyphenyl)-7-(naphthalen-1-yl)-5-oxo-5,6,7,8-tetrahydro-4H-chromene-3-carbonitrile), or dihydrokainate (DHKA) (all purchased from Tocris Bioscience Ellisville, MO, USA) were applied to astroglial cells 60 min before Glu.

Statistical analysis

Quantitative results are expressed as means ± standard errors (SE). Student's t-test was used to compare data, with $p<0.05$ considered significant.

Supporting Information

Figure S1 BrdU-incorporating cells in wild-type and MeCP2-null astrocytes. The top and bottom pictures show BrdU-incorporating (Green) and Hoechst-stained (Blue) cells, respectively, which were stained with the primary anti-BrdU antibodies, the secondary fluorescein-coupled antibodies, and Hoechst 33324. Negative controls received identical treatments, but were not exposed to BrdU. Representative pictures were used to accurately count the number of BrdU incorporated cells to assess the efficiency of astrocyte cell growth. Scale bar = 200 μm.
(EPS)

Figure S2 Concentration dependency of GS and EAAT1 expression in wild-type and MeCP2-null astrocytes treated with Glutamate. The astrocytes of each group were treated with 0.01–1.0 mM Glu for 12 h, and subsequently analyzed for expression of GS and EAAT1 by western blot analysis.
(EPS)

Figure S3 Purity of astroglial cultures from mouse brain. The purity of astroglial cultures was assessed by immunocytochemisty (**A**) and immunoblotting (**B**) using antibodies against glial fibrillary acidic protein (GFAP; astrocyte marker; Sigma-Aldrich), CD11b (microglial marker; Santacruz), or microtubule associated protein 2 (MAP2; neuronal marker; Sigma-Aldrich). **A.** Immunocytochemistry indicates that neither CD11b nor MAP2 were expressed in astrocyte cultures. Positive control indicates microglia and mouse ES-derived neural cells that stained with anti-CD11b and MAP2 antibodies, respectively. Scale bar = 100 μm. **B.** Western blot analysis of protein extracts from cultured astrocytes and mouse whole brain. Western blot analysis also confirmed that the cultured astrocytes expressed GFAP, but did not express CD11b and MAP2.
(EPS)

Figure S4 Optimization of the semi-quantitative RT-PCR assay. Total RNA extracted from neonatal mouse brain astrocytes was serially diluted (2.5, 5, 10, 20, and 40 ng RNA in lanes 1, 2, 3, 4, and 5, respectively), reverse-transcribed and used as control samples in semi-quantitative RT-PCR for GFAP (**A**), S100β (**B**), HPRT (**C**), EAAT1 (**D**), EAAT2 (**E**), and GS (**F**). PCR was carried out for indicated cycles using each of primer sets shown in Table 1. The amplified cDNA was electrophoresed in a 2% agarose gel containing ethidium bromide. NT, RT-PCR with no template.
(EPS)

Information S1 Supporting materials and methods.
(DOC)

Author Contributions

Conceived and designed the experiments: YO TT. Performed the experiments: YO CM TT. Analyzed the data: YO TT ET. Contributed reagents/materials/analysis tools: KK TM. Wrote the paper: YO TT.

References

1. Chahrour M, Zoghbi HY (2007) The story of Rett syndrome: from clinic to neurobiology. Neuron 56: 422–437.
2. Matsuishi T, Yamashita Y, Takahashi T, Nagamitsu S (2011) Rett syndrome: The state of clinical and basic research, and future perspectives. Brain Dev 33: 623–631.
3. Amir RE, Van den Veyver IB, Wan M, Tran CQ, Francke U, et al. (1999) Rett syndrome is caused by mutations in X-linked MECP2, encoding methyl-CpG-binding protein 2. Nat Genet 23: 185–188.
4. Guy J, Hendrich B, Holmes M, Martin JE, Bird A (2001) A mouse Mecp2-null mutation causes neurological symptoms that mimic Rett syndrome. Nat Genet 27: 322–326.
5. Chen RZ, Akbarian S, Tudor M, Jaenisch R (2001) Deficiency of methyl-CpG binding protein-2 in CNS neurons results in a Rett-like phenotype in mice. Nat Genet 27: 327–331.
6. Calfa G, Percy AK, Pozzo-Miller L (2011) Experimental models of Rett syndrome based on Mecp2 dysfunction. Exp Biol Med (Maywood) 236: 3–19.
7. Bienvenu T, Chelly J (2006) Molecular genetics of Rett syndrome: when DNA methylation goes unrecognized. Nat Rev Genet 7: 415–426.
8. Saywell V, Viola A, Confort-Gouny S, Le Fur Y, Villard L, et al. (2006) Brain magnetic resonance study of Mecp2 deletion effects on anatomy and metabolism. Biochem Biophys Res Commun 340: 776–783.
9. Ballas N, Lioy DT, Grunseich C, Mandel G (2009) Non-cell autonomous influence of MeCP2-deficient glia on neuronal dendritic morphology. Nat Neurosci 12: 311–317.
10. Maezawa I, Swanberg S, Harvey D, LaSalle JM, Jin LW (2009) Rett syndrome astrocytes are abnormal and spread MeCP2 deficiency through gap junctions. J Neurosci 29: 5051–5061.
11. Maezawa I, Jin LW (2010) Rett syndrome microglia damage dendrites and synapses by the elevated release of glutamate. J Neurosci 30: 5346–5356.
12. Okabe Y, Kusaga A, Takahashi T, Mitsumasu C, Murai Y, et al. (2010) Neural development of methyl-CpG-binding protein 2 null embryonic stem cells: a system for studying Rett syndrome. Brain Res 1360: 17–27.
13. Lioy DT, Garg SK, Monaghan CE, Raber J, Foust KD, et al. (2011) A role for glia in the progression of Rett's syndrome. Nature 475: 497–500.
14. Seifert G, Schilling K, Steinhauser C (2006) Astrocyte dysfunction in neurological disorders: a molecular perspective. Nat Rev Neurosci 7: 194–206.
15. Eroglu C, Barres BA (2010) Regulation of synaptic connectivity by glia. Nature 468: 223–231.
16. Sheldon AL, Robinson MB (2007) The role of glutamate transporters in neurodegenerative diseases and potential opportunities for intervention. Neurochem Int 51: 333–355.
17. Eid T, Williamson A, Lee TS, Petroff OA, de Lanerolle NC (2008) Glutamate and astrocytes–key players in human mesial temporal lobe epilepsy? Epilepsia 49 Suppl 2: 42–52.
18. Hamberger A, Gillberg C, Palm A, Hagberg B (1992) Elevated CSF glutamate in Rett syndrome. Neuropediatrics 23: 212–213.
19. Lappalainen R, Riikonen RS (1996) High levels of cerebrospinal fluid glutamate in Rett syndrome. Pediatr Neurol 15: 213–216.
20. Pan JW, Lane JB, Hetherington H, Percy AK (1999) Rett syndrome: 1H spectroscopic imaging at 4.1 Tesla. J Child Neurol 14: 524–528.
21. Horska A, Farage L, Bibat G, Nagae LM, Kaufmann WE, et al. (2009) Brain metabolism in Rett syndrome: age, clinical, and genotype correlations. Ann Neurol 65: 90–97.
22. Ward BC, Kolodny NH, Nag N, Berger-Sweeney JE (2009) Neurochemical changes in a mouse model of Rett syndrome: changes over time and in response to perinatal choline nutritional supplementation. J Neurochem 108: 361–371.

23. Viola A, Saywell V, Villard L, Cozzone PJ, Lutz NW (2007) Metabolic fingerprints of altered brain growth, osmoregulation and neurotransmission in a Rett syndrome model. PLoS One 2: e157.
24. Dunn HG, MacLeod PM (2001) Rett syndrome: review of biological abnormalities. Can J Neurol Sci 28: 16–29.
25. Naidu S, Kaufmann WE, Abrams MT, Pearlson GD, Lanham DC, et al. (2001) Neuroimaging studies in Rett syndrome. Brain Dev 23 Suppl 1: S62–71.
26. Colantuoni C, Jeon OH, Hyder K, Chenchik A, Khimani AH, et al. (2001) Gene expression profiling in postmortem Rett Syndrome brain: differential gene expression and patient classification. Neurobiol Dis 8: 847–865.
27. Setoguchi H, Namihira M, Kohyama J, Asano H, Sanosaka T, et al. (2006) Methyl-CpG binding proteins are involved in restricting differentiation plasticity in neurons. J Neurosci Res 84: 969–979.
28. Chen CJ, Liao SL, Kuo JS (2000) Gliotoxic action of glutamate on cultured astrocytes. J Neurochem 75: 1557–1565.
29. Lehmann C, Bette S, Engele J (2009) High extracellular glutamate modulates expression of glutamate transporters and glutamine synthetase in cultured astrocytes. Brain Res 1297: 1–8.
30. Shigeri Y, Seal RP, Shimamoto K (2004) Molecular pharmacology of glutamate transporters, EAATs and VGLUTs. Brain Res Brain Res Rev 45: 250–265.
31. Erichsen MN, Huynh TH, Abrahamsen B, Bastlund JF, Bundgaard C, et al. (2010) Structure-activity relationship study of first selective inhibitor of excitatory amino acid transporter subtype 1: 2-Amino-4-(4-methoxyphenyl)-7-(naphthalen-1-yl)-5-oxo-5,6,7,8-tetrahydro-4 H-chromene-3-carbonitrile (UCPH-101). J Med Chem 53: 7180–7191.
32. Deguchi K, Antalffy BA, Twohill LJ, Chakraborty S, Glaze DG, et al. (2000) Substance P immunoreactivity in Rett syndrome. Pediatr Neurol 22: 259–266.
33. Namihira M, Nakashima K, Taga T (2004) Developmental stage dependent regulation of DNA methylation and chromatin modification in a immature astrocyte specific gene promoter. FEBS Lett 572: 184–188.
34. Tsujimura K, Abematsu M, Kohyama J, Namihira M, Nakashima K (2009) Neuronal differentiation of neural precursor cells is promoted by the methyl-CpG-binding protein MeCP2. Exp Neurol 219: 104–111.
35. Jellinger K, Armstrong D, Zoghbi HY, Percy AK (1988) Neuropathology of Rett syndrome. Acta Neuropathol 76: 142–158.
36. Kim SY, Choi SY, Chao W, Volsky DJ (2003) Transcriptional regulation of human excitatory amino acid transporter 1 (EAAT1): cloning of the EAAT1 promoter and characterization of its basal and inducible activity in human astrocytes. J Neurochem 87: 1485–1498.
37. Yang Y, Gozen O, Vidensky S, Robinson MB, Rothstein JD (2010) Epigenetic regulation of neuron-dependent induction of astroglial synaptic protein GLT1. Glia 58: 277–286.
38. Ricciardi S, Boggio EM, Grosso S, Lonetti G, Forlani G, et al. (2011) Reduced AKT/mTOR signaling and protein synthesis dysregulation in a Rett syndrome animal model. Hum Mol Genet 20: 1182–1196.
39. Ushikoshi H, Takahashi T, Chen X, Khai NC, Esaki M, et al. (2005) Local overexpression of HB-EGF exacerbates remodeling following myocardial infarction by activating noncardiomyocytes. Lab Invest 85: 862–873.
40. Norenberg MD, Jayakumar AR, Rama Rao KV, Panickar KS (2007) New concepts in the mechanism of ammonia-induced astrocyte swelling. Metab Brain Dis 22: 219–234.
41. Takahashi T, Kawai T, Ushikoshi H, Nagano S, Oshika H, et al. (2006) Identification and isolation of embryonic stem cell-derived target cells by adenoviral conditional targeting. Mol Ther 14: 673–683.
42. Kawai T, Takahashi T, Esaki M, Ushikoshi H, Nagano S, et al. (2004) Efficient cardiomyogenic differentiation of embryonic stem cell by fibroblast growth factor 2 and bone morphogenetic protein 2. Circ J 68: 691–702.
43. Takeuchi H, Mizuno T, Zhang G, Wang J, Kawanokuchi J, et al. (2005) Neuritic beading induced by activated microglia is an early feature of neuronal dysfunction toward neuronal death by inhibition of mitochondrial respiration and axonal transport. J Biol Chem 280: 10444–10454.

nature COMMUNICATIONS

OPEN

ARTICLE

Received 21 Oct 2011 | Accepted 20 Feb 2012 | Published 27 Mar 2012

DOI: 10.1038/ncomms1755

FAD-dependent lysine-specific demethylase-1 regulates cellular energy expenditure

Shinjiro Hino[1], Akihisa Sakamoto[1], Katsuya Nagaoka[1], Kotaro Anan[1], Yuqing Wang[2], Shinya Mimasu[3,4], Takashi Umehara[3], Shigeyuki Yokoyama[3,4], Ken-ichiro Kosai[2] & Mitsuyoshi Nakao[1,5]

Environmental factors such as nutritional state may act on the epigenome that consequently contributes to the metabolic adaptation of cells and the organisms. The lysine-specific demethylase-1 (LSD1) is a unique nuclear protein that utilizes flavin adenosine dinucleotide (FAD) as a cofactor. Here we show that LSD1 epigenetically regulates energy-expenditure genes in adipocytes depending on the cellular FAD availability. We find that the loss of LSD1 function, either by short interfering RNA or by selective inhibitors in adipocytes, induces a number of regulators of energy expenditure and mitochondrial metabolism such as PPARγ coactivator-1α resulting in the activation of mitochondrial respiration. In the adipose tissues from mice on a high-fat diet, expression of LSD1-target genes is reduced, compared with that in tissues from mice on a normal diet, which can be reverted by suppressing LSD1 function. Our data suggest a novel mechanism where LSD1 regulates cellular energy balance through coupling with cellular FAD biosynthesis.

[1] Department of Medical Cell Biology, Institute of Molecular Embryology and Genetics, the Global Center of Excellence 'Cell Fate Regulation Research and Education Unit', Kumamoto University, 860-0811, Japan. [2] Department of Gene Therapy and Regenerative Medicine, Advanced Therapeutics Course, Graduate School of Medical and Dental Sciences, Kagoshima University, 890-8544, Japan. [3] RIKEN Systems and Structural Biology Center, Yokohama 230-0045, Japan. [4] Graduate School of Science, The University of Tokyo, 113-0033, Japan. [5] Core Research for Evolutional Science and Technology (CREST), Japan Science of Technology Agency, Tokyo, Japan. Correspondence and requests for materials should be addressed to S.H. (email: s-hino@kumamoto-u.ac.jp) or to M.N. (email: mnakao@gpo.kumamoto-u.ac.jp).

In response to environmental stimuli, epigenetic marks such as DNA and histone methylation may be dynamically added and removed for gene regulation during the transcriptional cycle[1,2]. Nutritional information may influence the epigenome by directly affecting the activities of epigenetic modifiers[3]. Notably, it has been reported that nutritional conditions in early life influence the susceptibility to chronic disorders, such as obesity and related metabolic diseases, later in life[4], suggesting underlying epigenetic mechanisms[5]. Thus, elucidating how nutritional information is transferred to the epigenetic machinery for the regulation of cellular metabolism, and the formation of the long-term metabolic phenotype is of great interest.

Lysine-specific demethylase-1 (LSD1, also known as KDM1A) is a member of the flavin-containing amine oxidase family that, in general, represses transcription by removing the methyl group from mono-methylated and di-methylated lysine 4 of histone H3 (H3K4)[6]. LSD1 is also involved in the demethylation of H3K9 when associated with some nuclear receptors[7], and in the demethylation of non-histone proteins such as p53, Stat3 and Dnmt1 (ref. 8–10), suggesting its contribution to selective biological processes. Indeed, genetic ablation of LSD1 in mice causes embryonic lethality[11], and LSD1-deficient embryonic stem cells had cell defects and global DNA hypomethylation[10], consistent with the important functions of LSD1.

Among numerous epigenetic factors, LSD1 is unique in that it utilizes flavin adenosine dinucleotide (FAD) as an essential cofactor for catalytic activities[12]. FAD serves as a coenzyme in many oxidative reactions including mitochondrial fatty acid β-oxidation and in the respiratory chain[13]. The majority of reported flavoenzymes localize to the mitochondria or cytoplasm, whereas LSD1 is one of a few flavoproteins in the nucleus. Another nuclear flavoprotein is apoptosis-inducing factor (AIF) that initially localizes to the mitochondrial inner membrane and translocates to the nucleus on oxidative stress or other proapoptotic stimuli, leading to DNA degradation[14], suggesting that AIF may transfer the mitochondrial metabolic information to the nucleus[15]. However, the biological significance of FAD-dependent LSD1 activities in metabolic regulation remains unknown.

In this study, we present direct evidence that the inhibition of LSD1, by short interfering RNA (siRNA)-mediated knockdown (KD) and by selective inhibitors, activates energy-expenditure genes by transcriptional and epigenetic mechanisms in adipocytes. Disruption of LSD1 function resulted in the de-repression of these genes leading to the activation of mitochondrial respiration and lipolysis in adipocytes. We further found that LSD1-mediated transcriptional repression is FAD-dependent, and that the disruption of cellular FAD synthesis exerted similar effects on the metabolic gene expression as the LSD1 inhibition. Importantly, the expression of LSD1-target genes was markedly repressed in high fat-exposed white adipose tissue (WAT), and could be reverted by LSD1 inhibition, indicating the involvement of LSD1 in metabolic adaptation *in vivo*. Our data shed light on an essential mechanism of energy utilization that might explain how cells determine their energy strategy depending on nutritional availability.

Results

LSD1 regulates energy-expenditure genes in adipocytes. During our investigations, we found that both LSD1 and its essential partner BHC80 (ref. 16), showed relatively high expression levels in WAT among metabolic tissues in mice (Fig. 1a; Supplementary Fig. S1a). In addition, adipogenic 3T3-L1 cells abundantly expressed BHC80, which was found to form a complex with LSD1 in these cells (Fig. 1b; Supplementary Fig. S1b,c). During adipogenesis, an increase in mono-methylated H3K4 was observed, which is indicative of the active regulation of H3K4 methylation in these cells (Supplementary Fig. S1d). To address the role of LSD1 function in adipose cells, we performed microarray-based expression analyses in 3T3-L1 cells. We disrupted LSD1 function by using specific siRNAs for LSD1 and BHC80 (Fig. 1c), as well as by using an LSD1 inhibitor, tranylcypromine (TC, also known as trans-2-phenylcyclopropylamine)[17–21], in adipocyte-differentiating 3T3-L1 cells. TC was initially identified as an inhibitor of monoamine oxidases (MAO) A and B[22], and was demonstrated to be a potent inhibitor of LSD1 (refs 17,18). In agreement with the transcriptional repressive activities of LSD1, 198 probe sets were commonly induced 1.5-fold or more by LSD1-KD, BHC80-KD and TC treatment (Fig. 1d; Supplementary Data 1). Focusing on the probe sets upregulated by LSD1-KD, we found significant enrichment of the probe sets that were similarly upregulated by TC ($P=2.8\times10^{-56}$ by χ^2 test), while only a few were oppositely regulated (Fig. 1e). A similar tendency was observed for the co-target probes of LSD1-KD and BHC80-KD ($P=8.0\times10^{-8}$ by χ^2 test). To clarify the biological relevance of the co-target genes, we used Gene set enrichment analysis[23] (Fig. 1f). Considering the physiological function of adipocytes, we found that many of the co-target genes were related to lipid metabolism and mitochondrial oxidative phosphorylation (OXPHOS). On the other hand, 95 probe sets were commonly downregulated more than 1.5-fold by LSD1-KD, BHC80-KD and TC. However, GSEA analysis of the downregulated genes under LSD1 inhibition identified no significantly enriched gene sets associated with energy metabolism (Fig. 1g; Supplementary Data 2).

By quantitative RT–PCR analyses, we confirmed that important regulators of energy metabolism (Fig. 2a), such as PPARγ coactivator-1α (PGC-1α), pyruvate dehydrogenase kinase 4 (PDK4), protein kinase A regulatory subunit 2 alpha (RIIalpha) and adipose triglyceride lipase (ATGL), were significantly upregulated (Fig. 2b,c; Supplementary Data 1). These gene products have been reported to have key roles in mitochondrial energy production and/or lipid mobilization[24–27]. Among them, elevated expression of PGC-1α is a hallmark of brown adipose tissue (BAT), which is specialized for consumptive metabolism for the purpose of thermogenesis[28]. Consistently, LSD1 inhibition induced the expression of fatty acid transporter 1 (FATP1), a critical regulator of BAT metabolism (Fig. 2b,c)[29,30]. The selective upregulation of the group of energy-expenditure genes was confirmed by the use of alternative siRNA against LSD1 (Fig. 2d,e). We also noticed that LSD1 inhibition did not affect the expression of the key adipogenic factors as well as the drivers of brown adipogenesis (Supplementary Table S1).

As TC is also a potent MAO inhibitor, we employed selective LSD1 inhibitors (SLIs) to discriminate whether the activation of the metabolic genes is attributable to specific inactivation of the enzymatic activity of LSD1. We used three SLIs, S2101, S2107 and S2111, which are structurally related to TC, but highly potent with substantially reduced affinity to MAOs (Supplementary Fig. S2a)[31]. All SLIs showed coherent effects against LSD1-target metabolic genes, suggesting a strong link between the enzymatic activity of LSD1 and energy metabolism (Fig. 2c). In addition, MAO inhibitors, pargyline and clorgyline[17], did not activate LSD1-target genes at the tested concentrations (Supplementary Fig. S2b). Consistently, IC50 values of LSD1 and MAO inhibitors correlate well with the activation of LSD1-target genes by these drugs (Supplementary Table S2). The expression microarray analysis, using the cells treated with SLIs, confirmed the selectivity of these drugs, and further emphasized the link between LSD1 enzymatic activity and metabolic gene regulation (Supplementary Fig. S2c,d). Collectively, these results indicate that LSD1 represses expression of the energy-expenditure genes in adipocytes.

LSD1 epigenetically represses energy-expenditure genes. To investigate the molecular mechanism of LSD1 action, we tested whether energy-expenditure genes are directly regulated by LSD1 in differentiating 3T3-L1 cells. Chromatin immunoprecipitation (ChIP) analysis revealed that LSD1 was specifically enriched near